Pattern Anal Applic (2013) 16:497–506
DOI 10.1007/s10044-011-0253-7

THEORETICAL ADVANCES

Joint segmentation and pairing of multispectral chromosome images

Yongqiang Zhao · Xiaolin Wu · Seong G. Kong · Lei Zhang

Received: 22 November 2010 / Accepted: 11 October 2011 / Published online: 29 October 2011

Abstract Automated segmentation of touching or overlapping chromosomes in a metaphase image is a critical step for computer-aided chromosomes analysis. Conventional chromosome imaging methods acquire single-band grayscale images, and such a limitation makes the separation of touching or overlapping chromosomes challenging. In the multiplex fluorescence in situ hybridization (M-FISH) technique, each class of chromosomes can bind with a different combination of fluorophores. The M-FISH technique results in multispectral chromosome images, which has distinct spectral signatures. This paper presents a novel automated chromosome analysis method to combine the pixel-level geometric and multispectral information with decision-level pairing information. Our chromosome segmentation method uses the geometric and spectral information to partition the chromosome cluster into three regions. There will be ambiguity when combining these regions into separated chromosomes by using only spectral and geometric information. Then a graph–theoretical pairing method is introduced to resolve any remaining ambiguity of the aforementioned segmentation process. Experimental results demonstrate that the proposed joint segmentation and pairing method outperforms conventional grayscale and multispectral segmentation methods in separating touching and overlapping chromosomes.

Keywords Multispectral imaging · Chromosome image segmentation · Shape decomposition · Homologue pairing

Y. Zhao (✉)
College of Automation, Northwestern Polytechnical University, Xi'an 710072, Shaanxi, China
e-mail: zhaoyq@nwpu.edu.cn; yongqzhao@gmail.com

X. Wu
Department of Electrical and Computer Engineering, The McMaster University, Hamilton, ON, Canada

S. G. Kong
Department of Electrical and Computer Engineering, Temple University, Philadelphia, PA 19122, USA

L. Zhang
Department of Computing, The Hong Kong Polytechnic University, Hung Hum, Kowloon, Hong Kong

1 Introduction

Chromosomes are genetic information carriers. When chromosomes are photographed during cell division, the images of these chromosomes contain crucial information about the health status of an individual. Chromosome analysis has been an important procedure in clinical and cancer cytogenetic studies [1, 2, 21, 24]. The classification of human chromosomes is called karyotype. Karyotyping is a useful tool to detect deviations from normal cell structure since abnormal cells may have an excess or a deficit of chromosome [21, 24]. In the past, karyotype used to be performed by trained cytogeneticist. This makes karyotype a time-consuming and expensive operation. There are medical and economic motivations to automate the karyotype generation process; however, automated image chromosome karyotyping (or classification) is still an open topic [3, 5, 6, 14].

As in many pattern recognition problems, the success of an automated karyotyping algorithm depends largely on the effectiveness of chromosomes' underlying feature representation scheme. With the development of multiplex fluorescence in situ hybridization (M-FISH) technology [2, 3, 5, 9–11, 20–23], apart from chromosome size, shape, morphology features, and chromosome banding patterns,

additional information provided by multiple spectrum in chromosome images makes it feasible to distinguish different chromosomes. The basic idea in M-FISH is that each chromosome is labeled by a unique combination of five fluors. An extra fluorophore, DAPI (4′6-diamidino-2-phenyl indole dihydrochloride), is counterstained to all chromosomes. In practice, fluorophore absorption is not binary and there is significant overlap between each of the fluorophore absorptions along with variability in signal strength. This leads to a non-trivial classification problem, especially in the context of overlapping regions [3, 9, 20–22]. Since chromosomes are somewhat opaque, and the detected fluorescence at a pixel may be the combination of its neighboring fluorescence, each pixel will involve the information from all overlapping chromosomes.

Automated segmentation of partially occluded and/or touching objects is an extremely challenging task. Chromosome images are subject to partial occlusion and/or touching with neighboring chromosomes. This is one of the major factors hindering automatic analysis [3]. There have been several segmentation methods developed to automate the analysis process in touching/overlapping chromosomes [1, 3, 6, 9, 12–14]. According to the information used, these methods can be classified into three groups: geometry-based methods, spectrum-based methods and combination of geometry- and spectrum-based methods.

Geometry-based methods assume that chromosome shapes alone are sufficient for the purpose of separation. These methods split the chromosome cluster into separated segments by using geometric characters (such as concave points, skeletons and so on), and then combine these segments into corresponding separated chromosomes. The reliability of these methods depends on two factors: splitting method and combination scheme. Agam and Dinstein [1] used concave points to construct all the possible separation lines. In their work, they determined potential chromosomes using rectangle hypothesis testing. Popescu [6] used the concepts of skeletons to decompose overlaps. Ji [28] also used the skeleton and cut points to decompose overlaps, and constructed a series of rules to classify the chromosomes. However, one problem is that the geometric information is not reliable in many cases to segment the touching and overlapping chromosomes, for example, two chromosomes touch by their short side or long side, forming a long chromosome as shown in Fig. 1a. The shape of chromosome cluster A and B is similar to that of chromosome C, and it is difficult to separate A and B by using contour information. The other problem is that geometric information is not sufficient to guide the combination of these segments. For example, in Fig. 1b, c, there are many ways to combine the segments, and using only the contour information is difficult to obtain correct segmentation results.

Spectrum-based methods assume that the spectral information is accurate enough to segment touching/overlapping chromosomes. Lot of work have been done in this field [2–4, 9, 11, 20–23]. Schwartzkopf et al. [3] proposed a joint classification and segmentation method by classifying every pixel to segment the touching/overlapping chromosomes. To improve the accuracy of pixel accuracy, Choi [21] introduced a new feature normalization method for M-FISH images that reduced the difference in the feature distributions among different images using the expectation maximization (EM) algorithm. To overcome the shortcoming of pixel-based classification, Karvelis [22, 23] performed the classification algorithm on homogeneous regions to improve the classification results. As the sensed fluorescence is not accurate and the chromosome is an opaque object, spectrum-based segmentation method is unreliable.

With the above analysis, geometry-based methods and spectrum-based methods have advantages and disadvantages. To make the overlapping and/or touching chromosomes separation more accurate, Choi [20] proposed a new separation method by using the spectral and geometric information. It utilized the pixel-based fuzzy-logic classifier to determine the cluster, and had the same shortcoming of pixel-based classification. The concave and convex points are used to divide the cluster into three basic elements: (1) cross-shaped cluster, (2) T-shaped cluster, and (3) I-shaped cluster. The touching/overlapping chromosomes are separated based on these three basic elements. It

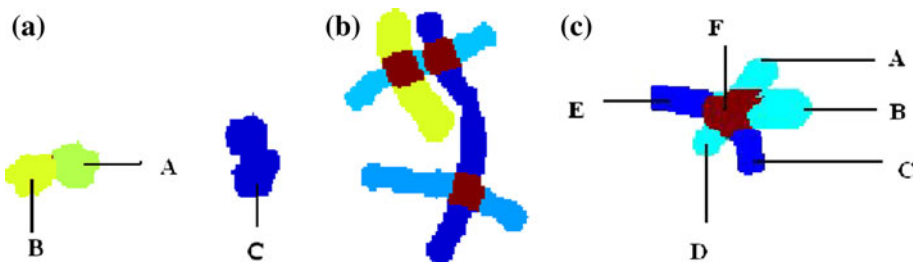

Fig. 1 Illustration of the ambiguity problems in chromosome segmentation. **a** On the *left* is the image composed by two chromosomes *A* and *B*, on the *right* is the one chromosome image, these two images have similar shape but different number of chromosomes; **b** a cluster with four chromosomes; **c** a cluster with three chromosomes and two chromosomes with same classes

is based on the assumption that every chromosome in cell cannot be separated into several parts according to the spectral information. But it is not true according to the Schwartzkopf's [3] research results. On the other hand, Choi's method cannot get the optimal results when two chromosomes with same class label are touched or overlapped. Biyani [4], Stanley [13] and Wu [26] utilized the prior information of human chromosome to classify and pair chromosomes, but this method can be used only on the well-separated chromosomes. Although previous methods have some shortcomings, they provide the incentive for this paper.

To separate more accurately the touching/overlapping chromosomes, we present a novel separation method based on the geometric and spectral information provided by M-FISH images and prior information of human chromosome. By effectively exploiting the spectral and geometric information, the segmentation of overlapping and touching chromosomes can be more accurate. We first detect the corner of overlapping/touching chromosomes using the curvature scale space method [7, 8], and partition the overlapping/touching chromosomes into three parts: end regions, intersection regions, and regular regions. Then we combine end regions, intersection regions and regular regions into potential chromosomes based on the spectral similarity. But there is ambiguity on choosing the optimal combination. For example, in Fig. 1c, regions A, B, and D have similar spectrum, there are six possibilities to form two chromosomes. Pixel-level information by itself cannot solve this problem, higher-level information have to be used to acquire the accurate combination. Here a graph–theoretical pairing method is introduced to resolve any remaining ambiguity of the aforementioned segmentation process. The main contribution of this paper is listed as follows:

1. The M-FISH imaging method provides abundant geometric and spectral information about the chromosomes, and there is complementary between them when separating the touching/overlapping chromosome. A novel overlapping/touching chromosome segmentation method is proposed based on the geometric and spectral information provided by M-FISH images.
2. A chromosome region segmentation method is applied to split the chromosome clusters into three regions based on convex and concave points.

The rest of the paper is organized as follows. In Sect. 2, by using convex and concave points of chromosome contour we present a chromosome region segmentation method to split the chromosome clusters into three regions. Then in Sect. 3, we present a homologous pairing method for proper region combination. In Sect. 4, experiments are carried out to validate the separation accuracy of touching/overlapping chromosome clusters in comparison with geometry-based and spectrum-based methods.

2 Extraction of primary shape elements

In general, the shape of a chromosome varies in different stages of mitosis. A chromosome may have different heights, widths and two or four arms, depending on whether some arms are joined. It may also bend to its centromere. (A centromere is a region of DNA typically found near the middle of a chromosome where two identical sister chromatids come in contact.) Although chromosomes may vary in shape and size, they all share a common basic shape, which is a rectangle that may contract and bend to one point [6, 24]. Based on such observations, the overlapping/touching chromosomes can be partitioned into some approximately rectangle-shaped segments, and then the original chromosomes can be represented as a combination of these segments without touching and overlapping. Next we describe how to obtain these segments in detail.

2.1 Definition of basic segments

A group of connected pixels can be regarded as a cluster, and it can be formed by one chromosome or multiple chromosomes, depending on whether there are overlapping and/or touching. The basic segment of a chromosome is rectangle, thus each cluster is formed as the combination of many rectangle segments. Given a cluster, we can extract the landmarks such as convex point and concave point via corner detection [18, 19]. Both the convex and concave points provide important information about the shape of chromosome. Unlike the method by Agam [1], which only uses the concave points to construct a series of parallel segmentation lines to separate the cluster, we use both the concave and convex points to separate the cluster into different regions. This can reduce the number of possible segments as well as the segment combination errors.

By computing the curvature of chromosome edge contours, and considering the local maxima and minima of curvature, we can get the corner points of chromosome [7, 8, 17, 18]. Here we define the convex point as end point (EP), and the concave point as cut point (CP). The EP and CP points can be used to extract the basic segments. Figure 2 shows two examples of EPs (black box) and CPs (white box). These two clusters, named as cluster 1 and cluster 2, respectively, will be used to illustrate the segment extraction process.

Based on the above definitions, one cluster can be divided into three basic parts termed as end region (ER), intersection region (IR) and regular region (RR). The ER is

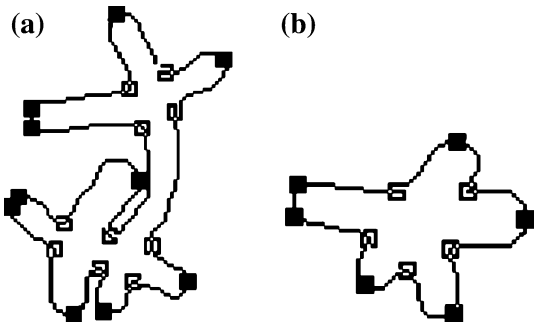

Fig. 2 Examples of end points and cut points of two clusters, where *black box* represents the EPs and *white box* represents the CPs: **a** cluster 1 is composed by four chromosomes; **b** cluster 2 is composed by three chromosomes

at the end of a chromosome and it is composed of EPs, CPs and boundary. The IR is only composed of four CPs. The RR, which is composed of CPs and the boundary, is used to represent the "smooth" part of the cluster. The following sections explain how to construct these regions.

2.2 Construction of end region (ER)

To construct an ER, the boundary of a cluster is traced from an end point, denoted by EP_k, in both clockwise and counter-clockwise directions to find the first two cut points, denoted by CP_i and CP_j. The line between these two cut points is defined as the end separation line $EL_{i,j}$. The boundary between EP_k and CP_i is represented as EC_{ki}, and the boundary between EP_k and CP_j is represented as EC_{kj}. The region encircled by EC_{ki}, EC_{kj}, and $EL_{i,j}$ is called the ER. We define by $EL = \{EL_{i,j} \mid \forall (CP_i, CP_j) \in ER\}$ the set of all ELs in the cluster.

Figure 3 shows an example of the ER construction process. The boundary of the cluster is traced from an EP (black box) to find the first two CPs (white box), and the EL is constructed by the two CPs. Referring to Fig. 2a, with the ten EPs in cluster 1 (the adjacent EPs will be merged—that means if two end points are closer than given threshold, these two end points are merged as one end point. Here the threshold is set as 10 points.), eight ERs can be constructed, as shown in Fig. 6a. For cluster 2 in Fig. 2b, there are six EPs and five ERs are constructed, which are shown in Fig. 6b.

2.3 Construction of intersection region (IR)

Since the shape of a chromosome is an enclosed region, the end separation line must be part of the intersection region, and the other parts of intersection region can be identified based on end separation line. So the whole intersection region can be divided into two parts: the first part, denoted by IR1, contains at least two end separation lines and the

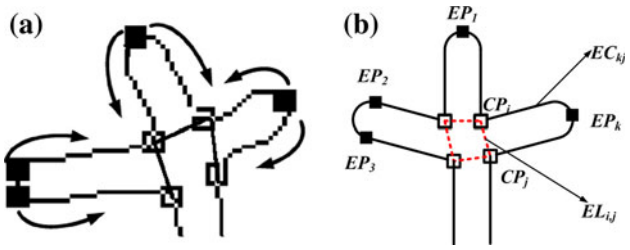

Fig. 3 Example of end region construction, boundary of the cluster is traced from one end point to find the first two concave points. **a** Example of end region construction; **b** example of end points (*EP*), cut points (*CP*), end lines (*EL*), and boundary between EP and CP (*EC*)

second part, denoted by IR2, contains at most one end separation line. Before explaining how to construct the IR1 and IR2, we define some basic relationships and operations between lines.

The nearly parallel relationship ρ_θ between the lines is defined as:

$$\rho_\theta = \Big\{ \big((CP_i, CP_j), (CP_m, CP_n) \big) \in (CP \times CP)^2 \;\Big|\; \mathrm{abs}\big(\Theta(CP_i, CP_j) - \Theta(CP_m, CP_n)\big) \le \tau_1 \Big\} \quad (1)$$

where $CP \times CP$ stands for all possible pairs of CPs considered, $(CP \times CP)^2$ represents all possible pairs of end separation lines considered, $\Theta(CP_i, CP_j)$ is the angle between the line (CP_i, CP_j) and the horizontal line. $\Theta(CP_i, CP_j)$ is normalized to the range $[0,\pi]$. $\tau_1$is the given threshold, to decide whether two lines are nearly paralleled, and set as 15°. The relation ρ_θ is reflective, antisymmetric and transitive.

Then the minimal and maximal operations in subset $X \subset CP \times CP$are defined as:

$$\min_\theta(X) = \{(CP_i, CP_j) \in X | \forall (CP_m, CP_n) \in X : \Theta(CP_i, CP_j) \le \Theta(CP_m, CP_n)\} \quad (2)$$

$$\max_\theta(X) = \{(CP_i, CP_j) \in X | \forall (CP_m, CP_n) \in X : \Theta(CP_m, CP_n) \le \Theta(CP_i, CP_j)\}. \quad (3)$$

End separation lines can be used to determine the location of IR. A pair of nearly parallel end separation lines determined by CP pairs (CP_i, CP_j) and (CP_m, CP_n) may specify an IR1 zone, if the following requirements are satisfied:

1. The line connecting the ends of the CP pairs (CP_i, CP_j) and (CP_m, CP_n) should be permitted separation lines, i.e., all pixels of line should be in cluster;
2. The difference of angles between the separation line and the two end separation lines should satisfy the minimal relationship $\min_\theta$.

   For the residual convex point sets to construct the IR2, any two arbitrary nearly parallel and permitted

separation lines should satisfy the above two conditions, and one additional requirement should be satisfied:

3. The separation lines should be continuous within the local region, i.e.:

$$(\Theta(\max_{\theta}(Y(\mathrm{CP}_i))) - \mathrm{Ang1} < \tau_2) \vee (\Theta(\max_{\theta}(Y(\mathrm{CP}_i))) - \mathrm{Ang2} < \tau_2) \quad (4)$$

where $\mathrm{Ang1} = \Theta(\mathrm{CP}_i, \mathrm{CP}_{i-l})$ and $\mathrm{Ang2} = \Theta(\mathrm{CP}_i, \mathrm{CP}_{i+l})$ are two angles for every cut point CP_i, l is the support width for every cut point CP_i, $Y(\mathrm{CP}_i)$ is the separation lines set whose one cut point is CP_i. τ_2 is the given threshold, and set as 35°.

Figure 4 shows the all possible separation lines in cluster 1 and cluster 2. Based on the proposed method, six pairs of separation lines are extracted from cluster 1, as shown in Fig. 6a. These six pairs of separation lines can be used to construct four IRs, which are shown in Fig. 6a. For cluster 2, four pairs of separation lines are extracted and four IRs can be constructed, which are shown in Figs. 6b. Figure 5 shows an illustration on how to construct the intersection region by using CP pairs $(\mathrm{CP}_i, \mathrm{CP}_j)$ and $(\mathrm{CP}_m, \mathrm{CP}_n)$. Although there are many potential choices on how to connect the dots $\mathrm{CP}_i, \mathrm{CP}_m$, CP_j and CP_n, but $(\mathrm{CP}_i, \mathrm{CP}_n)$ and $(\mathrm{CP}_j, \mathrm{CP}_m)$ (dashed lines in Fig. 5) do not satisfy the restriction of formulas (1) and (2).

2.4 Construction of regular regions (RR)

After determining all the ERs and IRs, the residual boundary parts and CPs in the cluster will be the basic elements to form RRs. RRs share the separation lines with IRs or share the end separation lines with ERs. So to construct the RR is to find the closed region formed by the boundary and separation lines. The RR of cluster 1 is shown in Fig. 6a and there is no RR in cluster 2.

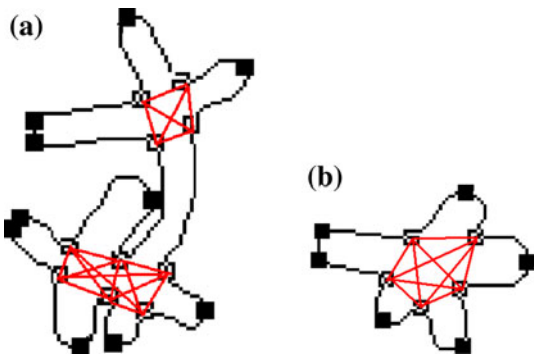

Fig. 4 Possible separation lines: **a** cluster 1, there are total 19 separation lines, but some separation lines cannot be used to construct intersection region; **b** cluster 2, there are total 9 separation lines

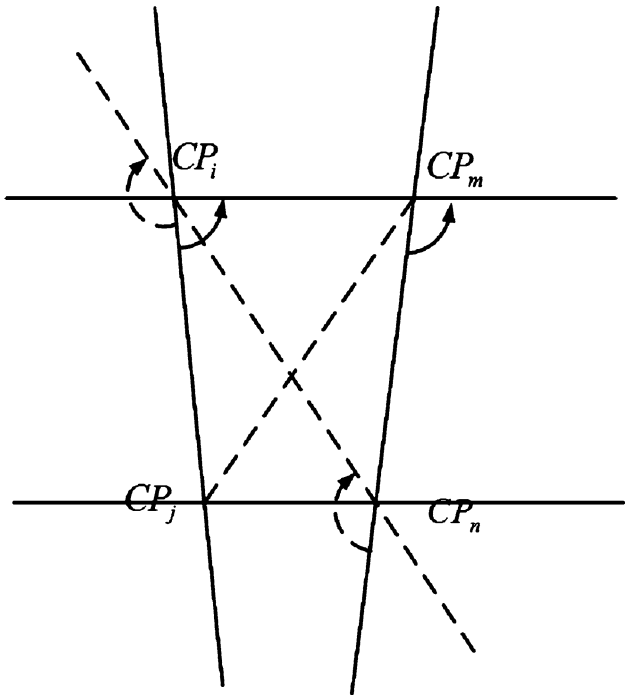

Fig. 5 An illustration on how to construct the intersection region by using CP pairs $(\mathrm{CP}_i, \mathrm{CP}_j)$ and $(\mathrm{CP}_m, \mathrm{CP}_n)$, where *straight and dashed lines* between $(\mathrm{CP}_i, \mathrm{CP}_m)$ and $(\mathrm{CP}_j, \mathrm{CP}_n)$ are the possible separation lines, but only *straight lines* satisfy the requirements (1) and (2)

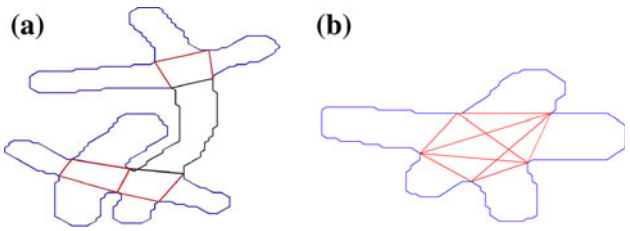

Fig. 6 The region separation results of **a** cluster 1 which is composed by eight end regions, three intersection regions and one regular region. **b** Cluster 2 is composed by five end regions and four intersection regions

After obtaining all the segments of a cluster, we focus on how to merge these segments properly to get the final segmented chromosome. Agam [1] proposed a verification method by testing whether the merged segments are satisfied with the rectangle assumption of chromosome's shape. This method only uses the local cluster's information. The next section describes the proposed segment merging method based on homologue pairing for the globally optimal combination of segments.

3 Joint segmentation and pairing

During the segment merging process, we combine end regions, intersection regions and regular regions into

potential chromosomes based on the spectral similarity. But there is ambiguity when touching/overlapping chromosomes with similar spectrum. On the other hand, it is difficult to decide whether the intersection regions should be combined with end regions, as one end region may be an individual chromosome. At the same time, the spectrum of intersection regions is decided by the top chromosome when several chromosomes are overlapping. By the affection of these factors, pixel-level method alone cannot acquire the optimal segments combination.

Here we give two examples to show the ambiguity in segments combination process. For example in Fig. 7a, if regions A, B, C and D have similar spectrum, there are three possibilities [(A + E+B, C + E + D), (A + E + D, B + E + C), (A + E + C, B + E + D)] to form two chromosomes. In Fig. 7b, if regions A, B and C have different spectrum, there are seven possibilities [(A + D, B + D, C + D), (A, B + D, C + D), (A + D, B, C + D), (A + D, B + D, C), (A, B, C + D), (A, B + D, C), (A + D, B, C)] to form three chromosomes. Pixel-level information alone cannot resolve these ambiguities, there is a need to introduce high-level information.

A normal human cell contains 22 homologous pairs of chromosomes and two sex chromosomes (two X for female or one X and one Y for male). The separated chromosomes (refer to Sect. 2 for chromosomes separation) should be paired into 23 homologous pairs (for female) or 22 homologous pairs plus two independent chromosomes (for male). Based on these constraints, the segments can be combined with the guidance of homologue pairing, and it can eliminate the combination ambiguities to acquire the optimal segments combination.

3.1 Homologue pairing

Any chromosome pairing can be identified with a permutation function $\tau(i)$ of integers $i \in \{1,2,\ldots,N\}$, where N is the number of chromosomes in one cell and $\tau(i) = j$ if and only if chromosomes X_i and X_j form a pair [4]. Obviously, $\tau(i) = j$ if and only if $\tau(j) = i$, and $\tau(i) \neq i$ for all i and j.

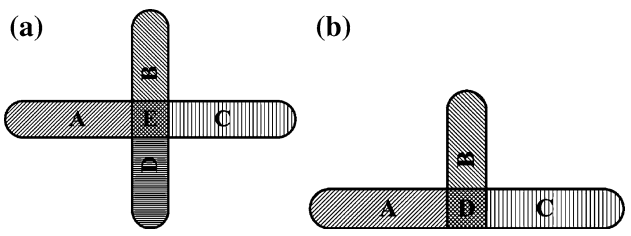

Fig. 7 Illustration of the ambiguity problems in chromosome segmentation. **a** There are five regions in the cluster, and according to the each region's characteristics, they can be combined in different ways; **b** there are four regions in the cluster

In pairing process, the whole chromosome set X is divided into two subsets $\tilde{X}$ and $\hat{X}$, such that $\tilde{X} \cup \hat{X} = X$, and for $\forall X_i \in \tilde{X}$, there is $X_{\tau(i)} \in \hat{X}$. The similarity of chromosome X_i and $X_{\tau(i)}$ can be measured by $S(X_i \cong X_{\tau(i)}; f_i, f_{\tau(i)})$, where $\cong$ is a binary relation. Then the problem of optimal pairing of chromosomes can be solved by maximizing the similarity measure function:

$$\tau_{\text{opt}} = \arg\max_{\tau} \sum_{i=1}^{N} S(X_i \cong X_{\tau(i)}; f_i, f_{\tau(i)}) \tag{5}$$

over all pairing τ. In order to solve the optimization problem of (5), we construct an undirected graph $G(X, E)$ with $|X| = N$ vertices and $|E| = M$ edges, where M is the number of chromosome pairs. Each vertex corresponds to a chromosome, and each edge to a pairing. The graph is weighted, and having the following constraints:

1. as every chromosome only belongs to one pair, no more than one edge can join the vertices;
2. for male, no edge can join the vertices corresponding X and Y chromosomes.

We associate a similarity measurement function S with an edge. For example, an edge $e = (X_i, X_j)$ has a weight $S(e) = S(X_i, X_j)$.The optimization of (5) can be solved by maximum-weight graph matching [15, 16],. The validity of the pairing results depends on the quality of the similarity measure function $S(X_i \cong X_{\tau(i)}; f_i, f_{\tau(i)})$. Next we discuss how to construct this function.

3.2 Construction of similarity measure function

The feature vector f_i for a chromosome can vary significantly among different types. In contrast, there is less variation between two chromosomes of the same class within a cell. Such observations inspire us toward a robust paradigm for chromosome pairing. As discussed in Sect. 1, the spectral and geometric features are important to tell different homologous pairs apart. For homologous pairs, their spectral and geometric difference should be small. Therefore, the similarity between two chromosomes can be measured based on their similarity in spectrum and geometry.

The spectrum similarity between two chromosomes X_i and X_j can be measured by using the Euclidean distance:

$$S_1(X_i, X_j) = \sqrt{\sum_{p=1}^{\text{PN}} (f_{i1}^p - f_{j1}^p)^T (f_{i1}^p - f_{j1}^p)} \tag{6}$$

where f_{i1} and f_{j1} are the spectral feature of chromosomes X_i and X_j, and PN is the number of pixels in chromosome. The relative size of chromosome X_i is defined as:

$$f_{i2} = \mathrm{Num}_i/\mathrm{Num}_T \quad (7)$$

where Num_i is the number of pixels belong to chromosome X_i, Num_T is the number of chromosomes pixels in the whole image. Then the size similarity measure can be defined as:

$$S_2(X_i, X_j) = \left\| f_{i2} - f_{j2} \right\|_2. \quad (8)$$

Based on the definition of spectrum and size measure functions, the final similarity measure function of chromosome X_i and X_j can be constructed as follows:

$$S(X_i \cong X_j) = S_1(X_i, X_j) \times S_2(X_i, X_j). \quad (9)$$

3.3 Joint segmentation and pairing algorithm

Based on the proposed segmentation and paring methods, the overlapping/touching chromosomes can be separated efficiently. The proposed segmentation–pairing algorithm is summarized as follows:

1. Preprocess the DAPI chromosome image to create the binary Mask by a thresholding procedure where the threshold value is selected using the Otsu's method [22, 27].
2. Smooth each chromosome object by using a 5×5 Gaussian filter to remove the noise.
3. Detect the cluster's corner, and partition the cluster into three parts: ERs, IRs and RRs, by using the algorithm proposed in Sect. 2.
4. Combine ERs, RRs and IRs into potential chromosomes based on the spectrum similarity and the continuity of chromosome that is calculated by (9).
5. For male cells, the pairing algorithm is used to choose the final segment results from potential chromosome sets. For female cells, two dummy chromosomes are first constructed according to the prior knowledge of relative size and spectrum of the X and Y chromosomes, and then the pairing algorithm is used to choose the final segmentation results from potential chromosomes set.
6. Final segmented chromosomes are the pairing result which is corresponding to the minimal cost.

4 Experimental results

The proposed method is tested on the Advanced Digital Imaging Research Company's M-FISH chromosome image database [25]. The database consists of 200 multispectral images with 517×645 pixels. Each pixel is represented as a 6-element vector: 5 multispectral channels plus the grayscale DAPI channel. The database also includes an karyotyped "ground truth" image according to the ISCN (International System for Human Cytogenetic Nomenclature) for each M-FISH image, so the segmentation results can be easily evaluated by accuracy [3, 22]. In this database, there is no annotation for 17 images which are reported as "difficult to karyotype" [25]. We excluded these images from the evaluation of our method.

The end points and cut points are detected by using the curvature of contour [7, 8, 18, 19]. We first compute the curvature of the edge [1], and consider those local maxima (minima) as initial end point (cut point), and remove one of end points which are very close. Then, mark residual end points with black box and cut points with white box. Two examples of detected end points and cut points are shown in Fig. 2. Within each separated end region, regular region or intersection region, there is great redundancy among pixels. To improve the accuracy of subsequent similarity measure, it is advantageous to compress the high-dimensional (pixel number) feature data into low dimensional representation such that irrelevant information can be reduced. Here we use the principal component analysis (PCA) [17] to extract the feature of each region, to make the every chromosome comparable, the first 30 component is preserved. In the experiments, we used the maximum flow method to solve the maximum-weight graph matching problem, maximum flow method is a basic means to solve the graph matching problem [15, 16].

Figure 8 shows an example of image (A020402) segmented with the proposed method. Figure 8a shows the primary shape extraction results of four clusters and Fig. 8b is its joint segmentation and pairing result. Compared with the hand-labeled karyogram result in Fig. 8c, the clusters 1, 2, 3, 4 are segmented properly.

For those abnormal cells with odd number chromosomes, one dummy chromosome is added according to the prior knowledge of spectrum and size. That means for these kinds of cells, to utilize the proposed algorithm, the prior information about which chromosome is absent/redundant must be known. At the same time, there are chromosome translocations in some cells, they will affect the touching/overlapping chromosomes' separation performance. If the chromosome translocation region is very small compared with the size of chromosome, the touching/overlapping chromosomes can be separated correctly, but the translocation abnormality will not be detected. In this situation, previous spectrum-based segmentation also failed, as it is difficult to distinguish this kind of translocation with noise [3]. If the chromosome translocation region is large compared with the size of chromosome, there will be some errors when separating touching/overlapping chromosomes. If the matching algorithm will not converge to a threshold in given iteration number, the whole pairing process is a failure and we mark this cell as an abnormal cell, which means there are some translocations in this cell.

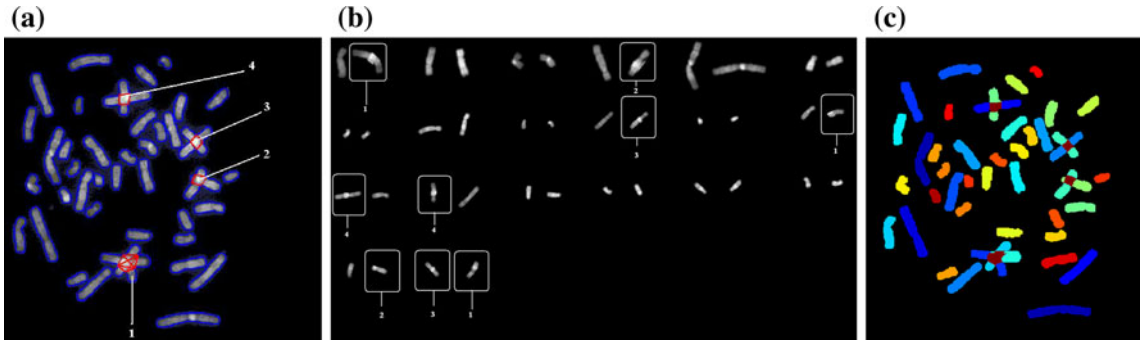

Fig. 8 Example of segmentation and pairing results. **a** Primary shape extraction results of four clusters; **b** joint segmentation and pairing result; **c** hand-labeled karyogram result

Table 1 Cluster separation results

Number of chromosomes in a cluster	Correct separation (%)	Erroneous separation (%)
2	80	13
3	74	18
≥4	71	23
Total	75	18

Table 2 Percentage of correct segmentation for various cluster types by using different algorithm

	This paper's algorithm (%)	ML method (%)	Geometric separation (%)
Touches	79	77	62
Overlaps	73	34	41

If the cell is marked as abnormal, the final combination results will be only based on the spectral similarity, as there are no converging matching results. It will need the help of cytogeneticist to analysis the chromosomes in the marked abnormal cell.

The results of cluster separation results by the proposed method are listed in Table 1. As could be seen from Table 1, 75% of clusters are separated correctly. The segmentation results by using different algorithm are shown in Table 2. Joint segmentation and pairing method correctly decomposed a much higher percentage of touches compared to the maximum likelihood (ML) based joint segmentation-classification method [3] and geometric separation method [1]. If two chromosomes of the same class touch or overlap, there is no way to determine their boundary with multispectral information alone. Geometric information can be used to separate these chromosomes. ML method segmentation accuracy is inherently dependent on pixel classification accuracy. Pixel classification rates vary widely through the M-FISH image dataset [3]. All these factors influence segmentation performance by using ML method. On the other hand, the geometric information is not so reliable in many cases to segment the touching and overlapping chromosomes, such as two chromosomes touching by their short side or long side forming a long chromosome. Joint segmentation and pairing method utilizes the spectral and geometric information jointly, it can overcome the shortcomings of segmentation methods which only uses spectral information or geometric information alone. And all the information used in joint segmentation and pairing method comes from single cell's image, not from the whole image dataset, and ignores the signal's variation of different cells.

From the experimental results on the M-FISH dataset, we conclude that most of the chromosomes that are incorrectly segmented by the proposed algorithm fall into the following two cases:

1. In the case that several chromosomes are clustered together, the corner cannot be detected correctly, and hence the corresponding ER and IR cannot be constructed correctly. This will make the segmentation fail. One typical example is cluster in Fig. 9.
2. In the case that there are some translocations in the cells and the region of translocation is larger than about 30–40 pixels, the pairing method will not converge to given threshold. We can only mark the abnormality of this cell, but the result of segmentation and pairing is not accurate.

To testify the pairing accuracy, we label the paired chromosome based on their spectrum and compare the classification accuracy with other methods. Table 3 shows a comparison of several different classification algorithms. Schwartzkopf et al. [3] proposed a joint segmentation and classification method that employs pixel-by-pixel classification schemes; the classification will be dominated by noisy painting in-homogeneities. This is obvious by the misclassifications errors produced by the pixel-by-pixel algorithm. Choi et al. [20], Cao et al. [29]. and Wang et al. [15] also proposed M-FISH chromosome classification, and

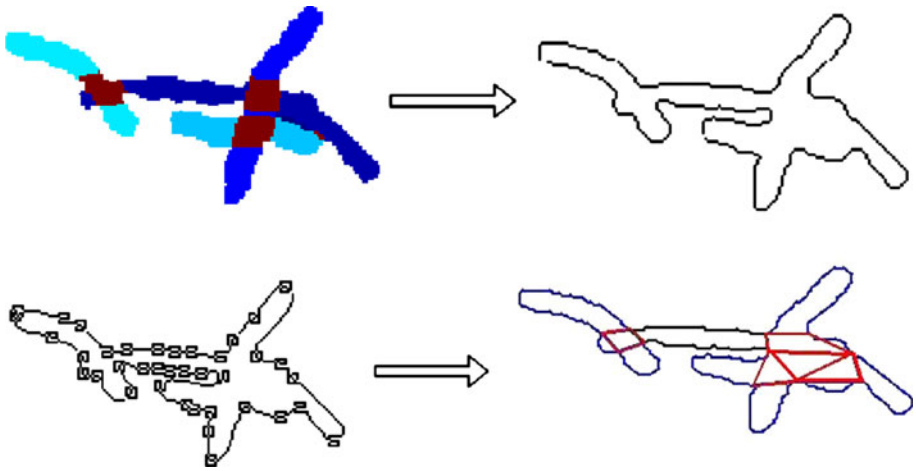

Fig. 9 An example failure case of the proposed method. *Top* four chromosomes clusters and corresponding detected edge, there is some errors on edge detection; *bottom* the detected concave and convex points and corresponding constructed regions, edge detection errors cause the mistakes of region construction

Table 3 Comparison of the proposed method and other methods that appeared in the literature in terms of chromosome classification accuracy

Method	No. of images	Average chromosome pixel classification (%)
Schwartzkopf et al. [3]	183	68.0
Karvelis et al. [22]	183	82.5
Cao et al. [29]	120	84.1
Choi et al. [20]	10	97.1
Wang et al. [15]	5	87.5
This work	183	89.2

got good results on part of the ADIR M-FISH dataset. They also employed pixel-by-pixel classification schemes. Karvelis et al. [22] presented a multichannel watershed based method, where classification was based on the spectrum of all pixels belonging to a specific region. Analyzing the classification results in Table 3 demonstrated that the classification algorithm proposed in this paper got the highest classification accuracy tested on all datasets. The algorithm proposed by Choi get 97.1% classification accuracy, but it only tested on 10 images. As the graph matching is used in the proposed algorithm to improve the classification accuracy, time consumed is higher than other algorithm. The average classification time is 180 s on a Pentium P4 2.33 GHz PC, with 2G RAM by using Matlab 2009. Under the same condition, Schwartzkopf et al.'s [3] algorithm takes 170 s, and Karvelis et al.'s [22] algorithm 120 s.

5 Conclusion

This paper presented a joint segmentation and pairing scheme for touching and overlapping chromosomes by using both the pixel-level geometric and spectral information and decision-level pairing information. Unlike the previous geometric separation method, the proposed approach uses the concave and convex points of cluster to separate the cluster into three regions: ER, IR and RR. Then these regions are combined into potential chromosomes according to the spectrum similarity measure and the continuity of chromosome. Finally, we use the homologous pairing method to determine which potential chromosome is chosen. Experimental results demonstrated the superior performance of the proposed method to the previous methods in terms of segmentation and paring accuracy.

Acknowledgments This work is supported by the National Nature Science Foundation of China under Grant No. 61071172, 60602056, China Scholarship Council and Aviation Science Funds 20105153022, and Sciences Foundation of Northwestern Polytechnical University No. JC200941.

References

1. Agam G, Dinstein IH (1997) Geometric separation of partially overlapping nonrigid objects applied to automatic chromosome classification. IEEE Trans Pattern Anal Mach Intel 19(11): 1212–1222
2. Maierrhofer C, Jentsch I, Lederer G et al (2002) Multicolor FISH in two and three dimensions for clastogenic analysis. Mutagenesis 17(6):523–527
3. Schwartzkopf WC, Bovik AC, Evans BL (2005) Maximum likelihood techniques for joint segmentation-classification of multi-spectral chromosome images. IEEE Trans Med Imaging 24(12):1593–1610
4. Biyani P, Wu X, Sinha A (2005) Joint classification and pairing of human chromosomes. IEEE Trans Comput Biol Bioinforma 2(2):102–109
5. Shah S (2005) Multispectral integration for segmentation of chromosome images. In: CAIP 2005, LNCS 3691:506–513
6. Popescu M, Gader P, Keller J et al (1999) Automatic karyotyping of metaphase cells with overlapping chromosomes. Comput Biol Med 29(1):61–82
7. Mokhtarian F, Suomela R (1998) Robust image corner detection through curvature scale space. IEEE Trans Pattern Anal Mach Intel 20(12):1376–1381

8. He XC, Yung NHC (2004) Curvature scale space corner detector with adaptive threshold and dynamic region of support. In: ICPR 2004. 2:791–794
9. Choi H, Castleman KR, Bovik AC (2006) Segmentation and fuzzy-logic classification of M-FISH chromosome images. In: IEEE international conference on image processing, 2006, pp 69–72
10. Garini Y, Gil A, Bar-Am I et al (1999) Signal to noise analysis of multiple color fluorescence imaging microscopy. Cytometry 35:214–226
11. Gariniy Y, Macvillez M, du Manoir S et al (1996) Spectral karyotyping. Bioimaging 4:65–72
12. Lerner B (1998) Toward a completely automatic neural-network-based human chromosome analysis. IEEE Trans Trans Syst Man Cybern Part B 28(4):544–552
13. Stanley RJ, Keller JM, Gader P, Caldwell CW (1998) Data-driven homogue matching for chromosome identification. IEEE Trans Med Imaging 17(3):451–462
14. Carothers A, Piper J (1994) Computer-aided classification of human chromosomes: a review. Stat Comput 4(3):161–171
15. Wang Y, Castleman KR (2005) Normalization of multicolor fluorescence in situ hybridization (M-FISH) images for improving color karyotyping. Cytometry 64:101–109
16. Almohamad HA, Duffuaa SO (1993) A linear programming approach for the weighted graph matching problem. IEEE Trans. Pattern Anal Mach Intel 15(5):522–525
17. Ramanath R, Snyder WE, Qi H (2003) Eigenviews for object recognition in multispectral imaging systems. In: Proceedings of the 32nd applied imagery pattern recognition workshop (April 2003), pp 33–38
18. Tang Y, Chen R, Qiu YH (2003) An effective stroke extraction model for chinese characters. In: Proceeding of the second international conference on machine learning and cybernetrics, pp 3193–3198
19. Nishida H, Mori S (1992) Algebraic description of curve of structure. IEEE Trans Pattern Anal Mach Intel 14(5):516–533
20. Choi H, Bovik AC, Castleman KR (2006) Maximum-likelihood decomposition of overlapping and touching M-FISH chromosomes using geometry, size and color information. In: Proceedings of the 28th IEEE EMBS annual international conference, 2006, pp 3130–3133
21. Choi H, Castleman KR, Bovik AC (2008) Feature normalization via expectation maximization and unsupervised nonparametric classification for M-FISH chromosome images. IEEE Trans Med Imaging 27(8):129–136
22. Karvelis PS, Tzallas AT, Fotiadis DI et al (2008) A multichannel watershed based segmentation method for multispectral chromosome classification. IEEE Trans. Med Imaging 27(5):697–708
23. Karvelis PS, Fotiadis DI (2008) A region based decorrelation stretching method: application to multispectral chromosome classification. In: 15th IEEE international conference on image processing, pp 1456–1459
24. Thompson M, McInnes R, Willard H (1991) Genetics in medicine. Saunders, Kingston
25. The ADIR M_FISH Image Database (online)
26. Wu X, Dumitrescu S, Biyani P et al (2005) Fast chromosome karyotyping by auction algorithm. Int J Bioinforma Res Appl 1(3):351–362
27. Otsu N (1979) A threshold selection method from grey-level histograms. IEEE Trans On Syst Man Cybern 19(1):62–66
28. Ji L (1994) Fully automatic chromosome segmentation. Cytometry 17:196–208
29. Cao H, Wang Y (2011) Segmentation of M-FISH images for improved classification of chromosomes with an adaptive Fuzzy C-Means Clustering Algorithm. In: IEEE international symposium on biomedical imaging: from nano to macro, 2011, pp 1442–1445